



Showcasing a minireview article from Professor Aiguo Wu's team, Cixi Institute of Biomedical Engineering, Ningbo Institute of Materials Technology and Engineering, Chinese Academy of Sciences, Ningbo, 315201, PR China.

Navigating nMOF-mediated enzymatic reactions for catalytic tumor-specific therapy

Tailored to the specific tumor microenvironment (TME), emerging nMOF-based enzymatic nanocatalysts, (i) nMOFs with intrinsic enzyme-mimicking performance, and (ii) enzyme- and (iii) nanzyme-engineered nMOFs, have secured their places as "magic bullets" producing dramatic and tumor-specific therapeutic outcomes. This minireview concentrates on the advances and recent developments in various nMOF-mediated enzymatic reactions toward the internal stimuli of the TME (acidosis, high-glucose conditions, and the overproduction of glutathione, hydrogen peroxide and lactate). The challenges and insights for accelerating the exploration of nMOFs as catalytic tumor-specific therapeutic agents are also put forward.

### As featured in:



See Tianxiang Chen, Aiguo Wu *et al.*, *Mater. Horiz.*, 2020, **7**, 3176.



Cite this: *Mater. Horiz.*, 2020, 7, 3176

Received 31st July 2020,  
Accepted 26th August 2020

DOI: 10.1039/d0mh01225d

[rsc.li/materials-horizons](http://rsc.li/materials-horizons)

## Navigating nMOF-mediated enzymatic reactions for catalytic tumor-specific therapy

Chuang Liu, <sup>†ab</sup> Junlie Yao, <sup>†ab</sup> Jiapeng Hu, <sup>†ab</sup> Ozioma Udochukwu Akakuru, <sup>†ab</sup> Shan Sun, <sup>a</sup> Tianxiang Chen<sup>\*a</sup> and Aiguo Wu <sup>\*a</sup>

Nanoscale metal–organic frameworks (nMOFs), exhibiting highly designable structures, multiple surface functionalities, and well-defined porous apertures, have spurred intensive research as superior anti-tumor candidates with great promise. Tailored to the specific tumor microenvironment (TME), emerging nMOF-based enzymatic nanocatalysts, (i) nMOFs with intrinsic enzyme-mimicking performance, and (ii) enzyme- and (iii) nanozyme-engineered nMOFs, have secured their place as “magic bullets”, producing dramatic and tumor-specific therapeutic outcomes. Here, this review concentrates on the advances and recent developments in various nMOF-mediated enzymatic reactions toward the internal stimuli of the TME (acidosis, high-glucose conditions, and the overproduction of glutathione, hydrogen peroxide, and lactate). We also set forth challenges and offer insights relating to accelerating the exploration of nMOFs as catalytic tumor-specific therapeutic agents.

### 1. Introduction

Over the past several decades, the fast development of tumor-associated biology has witnessed significant progress for a

<sup>a</sup> Cixi Institute of Biomedical Engineering, CAS Key Laboratory of Magnetic Materials and Devices, Zhejiang Engineering Research Center for Biomedical Materials, Ningbo Institute of Materials Technology and Engineering, Chinese Academy of Sciences, Ningbo, 315201, P. R. China. E-mail: chentx@nimte.ac.cn, aiguo@nimte.ac.cn

<sup>b</sup> University of Chinese Academy of Sciences, Beijing, 100049, P. R. China

† These authors contributed equally.



Chuang Liu

Chuang Liu received his BS degree from China University of Mining and Technology in 2016. He then became a PhD candidate under the supervision of Prof. Aiguo Wu at Ningbo Institute of Materials Technology and Engineering (NIMTE), Chinese Academy of Sciences (CAS). He is also a joint PhD student in Prof. Wei Tao's group (Omid C. Farokhzad Lab) at the Center for Nanomedicine, Brigham and Women's Hospital, Harvard Medical School, Boston, USA.



Tianxiang Chen

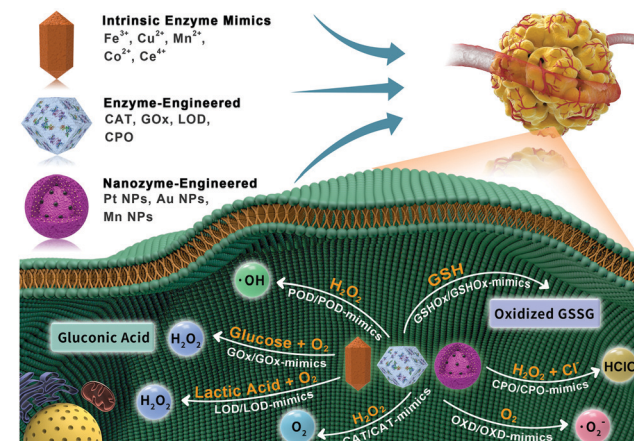
better understanding of tumor heterogeneity. The specific microenvironment and the biological microstructure of a tumor have, to some extent, stimulated a revolution in tumor theragnostics. In particular, the tumor microenvironment (TME),<sup>1</sup> featuring aberrant physiochemical properties and mal-adjusted biosynthetic intermediates, including up-regulated biomolecules (e.g. hydrogen peroxide ( $H_2O_2$ ), glutathione (GSH), glucose and lactate), and metabolic conditions (e.g. acidosis and hypoxia), have triggered the explosive attention on *in situ* biochemical reactions with appreciable anti-tumor efficiency.<sup>2</sup>

Tianxiang Chen received his PhD degree in 2012 from Donghua University. He is a senior engineer at NIMTE, CAS. His research focuses on the synthesis, functions, and characterization of nano-biomaterials. He is also committed to the preparation and industrialization of MRI contrast agents to diagnose major diseases (cancer, cardiovascular diseases, and other neurological diseases) at an early stage.

In this way, efforts to transfer such appealing features have led to the construction of TME-catalytic nanoreactors, which enable the generation of toxic reactive oxygen species (ROS), the production of oxygen to benefit tumor hypoxia relief-enhanced therapeutic strategies, and energy consumption-induced starvation therapy. Driven by the development of 'nanocatalytic medicine',<sup>3,4</sup> numerous nanoplatforms with intriguing catalytic performances have shown satisfactory values in tumor therapy.<sup>5</sup> Among these, nanoscale metal-organic frameworks (nMOFs) consisting of metal ions and organic ligands,<sup>6–11</sup> have shown significant advances in tumor theranostics.<sup>12–15</sup>

Recently, nMOFs and nMOFs-based nanocatalysts have been employed as catalytic nanomedicines for tumor-specific therapy. To start with, nMOFs with intrinsic enzyme-mimicking performances have been discovered with excellent catalytic activities. For instance, the unique metal ions (*e.g.* iron, copper, manganese, cobalt, and cerium) of nMOFs can provide abundant catalytic sites and promote the diffusion of a variety of substrates by serving as peroxidase (POD)-, catalase (CAT)-, oxidase (OXD)-, and glutathione oxidase (GSHOx)-mimics. Next, leveraging the various functionalization strategies of nMOFs, natural enzymes such as catalase, glucose oxidase (GOx), lactate oxidase (LOD) and chloroperoxidase (CPO) have been widely applied to decorate the surface of nMOFs *via* covalent conjugation or electrostatic interactions. However, the feasibility of such enzyme-engineered nMOFs as catalytic nanomedicines is mainly hindered by their potentially reduced catalytic activities with regard to leaching and aggregation processes.<sup>16</sup> Last, compared with natural enzymes, nanozymes (artificial enzymes) with improved stability toward harsh environments may provide great opportunities to fabricate designable nanozyme-engineered nMOFs.<sup>17</sup> Nevertheless, their relatively lower catalytic specificities and efficiencies remain stumbling blocks for nanozymes.<sup>18</sup>

On the basis of extensive experimental exploration, nMOFs-based enzymatic nanocatalysts, including (i) nMOFs with intrinsic enzyme-mimicking performance, (ii) enzyme- and (iii)



Scheme 1 nMOF-mediated enzymatic substrate transformations for catalytic tumor-specific therapy.

nanozyme-engineered nMOFs, have been highlighted with superiority for catalytic tumor-specific therapy (Scheme 1). This minireview focuses on the current representative modalities of emerging nMOFs-based nanocatalysts, hitherto applied in enzymatic reactions for tumor-specific therapy. Then, current challenges are presented alongside future prospects. Hopefully, it will spur further biomedical research into nMOFs and nanocatalytic medicine.

## 2. nMOFs with intrinsic enzyme-mimicking performance

Compared with traditional catalytic nanomaterials, nMOFs have some potential advantages with regard to their chemical diversity, high cargo-loading capacity, and adjustable enzyme-mimicking performance by selecting metal centers and functionalized organic ligands.<sup>19–21</sup> In addition, the channel structure of nMOFs can provide a large number of catalytic sites, and promote the diffusion of a variety of substrates, which contributes to their fascinating catalytic activity. For instance, closely related to the Fenton reaction or Fenton-like reaction, the POD-mimicking activity of nMOFs has received wide attention. In addition CAT- and GSHOx-mimicking activities of nMOFs have also been extensively studied. In this section, representative enzyme-mimicking nMOFs, including iron (Fe)-, copper (Cu)-, manganese (Mn)-, cobalt (Co)- and cerium (Ce)-based nMOFs, will be presented.

### 2.1 Iron-based nMOFs

Fe-based nMOFs have been proven to be effective for therapeutic and diagnostic applications, including Fe-deficiency treatment, drug delivery and magnetic resonance imaging.<sup>22</sup> In the field of catalysis, the chemical reactions between  $\text{Fe}^{2+}/\text{Fe}^{3+}$  and  $\text{H}_2\text{O}_2$  may generate ROS directly and do not require light triggering.<sup>23,24</sup>

Recently, the POD-mimicking activity of Fe-based nMOFs has been well studied. Liu *et al.* loaded ABTS (2,2'-azino-bis(3-ethylbenzothiazoline-6-sulfonic acid)) into POD-mimicking



Aiguo Wu

*Aiguo Wu received his PhD degree in 2003 from Changchun Institute of Applied Chemistry, CAS, supervised by Prof. Erkang Wang and Prof. Zhuang Li. He stayed at the University of Marburg (Prof. Norbert A. Hampp's group) from 2004–2005, California Institute of Technology (Prof. Ahmed Zewail's group) from 2005–2006, and Northwestern University (Prof. Gayle E. Woloschak group) from 2006–2009. He is currently a full professor at NIMTE and the director of Cixi Institute of Biomedical Engineering, CAS. His lab focuses on nanoprobes for the early diagnosis and therapy of diseases.*

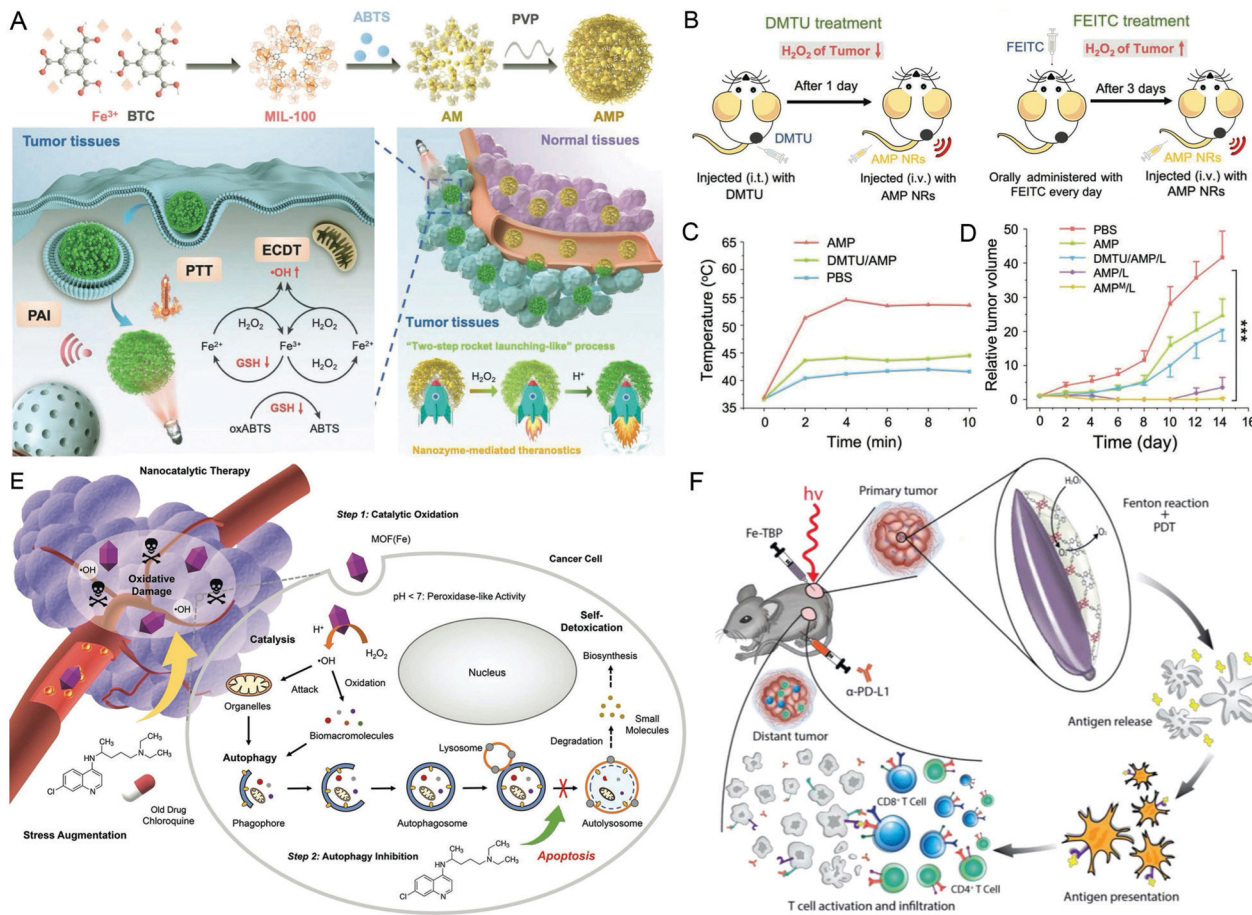


**Fig. 1** Iron-based nMOFs. (A) The preparation procedure and a schematic illustration of POD-mimicking AMP NRs-mediated theranostics, and (B) the tumor-specific photoacoustic imaging (PAI) ability of AMP NRs. (C) Photothermal curves and (D) the relative tumor volume in diverse groups. Reproduced with permission.<sup>25</sup> Copyright: 2019, Wiley-VCH. (E) A schematic illustration of the therapeutic concept of NH<sub>2</sub>-MIL-88B nMOFs. Reproduced with permission.<sup>26</sup> Copyright: 2020, Wiley-VCH. (F) A schematic illustration of immunogenic photodynamic therapeutics of Fe-TBP. Reproduced with permission.<sup>27</sup> Copyright: 2018, American Chemical Society.

nMOFs (MIL-100), abbreviated as AMP NRs, for H<sub>2</sub>O<sub>2</sub>-activated and acid-enhanced synergistic treatment (Fig. 1A–D).<sup>25</sup> The AMP NRs possessed excellent pH-sensitive catalytic activity for the generation of highly oxidizing hydroxyl radicals (•OH) and also had a photothermal therapy (PTT) property. By disrupting intracellular GSH credited to ABTS, AMP NRs could achieve effective ablation of tumors with minimal damage to normal tissues. In another study, NH<sub>2</sub>-MIL-88B nMOFs were reported for nanocatalytic tumor therapy combined with a pharmacological autophagy inhibition strategy (Fig. 1E).<sup>26</sup> In this nanoagent, chloroquine (CQ), a classical autophagy inhibitor, was employed for efficient blockage of the self-protective pathway (e.g., oxidative damage mitigation) in tumor cells after the primary •OH attack triggered by nMOFs. The rationally designed synergistic effect between nanocatalytic therapy and autophagy inhibition was proved to amplify tumor-specific oxidative damage.

CAT-mimicking activity is another interesting property of Fe-based nMOFs, which has become the focus of various research studies. In this regard, a novel nanophotosensitizer of Fe-TBP nMOFs (Fig. 1F) was synthesized to mediate catalytically-enhanced photodynamic therapeutic (PDT) treatment and

immunotherapy.<sup>27</sup> The Fe-TBP nMOFs could convert H<sub>2</sub>O<sub>2</sub> into oxygen (O<sub>2</sub>) to afford effective hypoxia relief-induced PDT, thus improving the efficacy of immune checkpoint blockade (ICB) and promoting abscopal effects, further enhancing the α-PD-L1 (anti-programmed death-ligand 1) treatment and could induce more than 90% regression of tumors. In a recent study conducted by our group, an Fe<sup>3+</sup>-based porous coordination network (PCN) was prepared to encapsulate paclitaxel (PTX) for combination tumor therapy.<sup>28</sup> The Fe<sup>3+</sup> offered both catalytic and magnetic resonance imaging functions, which could sensitize the O<sub>2</sub>-dependent PDT and monitor therapeutic responses.

## 2.2 Copper-based nMOFs

In the past few years, Cu-based nMOFs that were employed for various applications have been extensively studied. The chemical reactions triggered by Cu-based nMOFs show excellent performance in both kinetics and energy. For instance, the Fenton-like reaction catalyzed by the POD-mimicking activity of cuprous ions (Cu<sup>+</sup>/Cu<sup>2+</sup>) can be effective even in a weak acid medium, and the optimum reaction rate can reach about 160 times more than that of ferrous ions.<sup>29</sup> Additionally, the

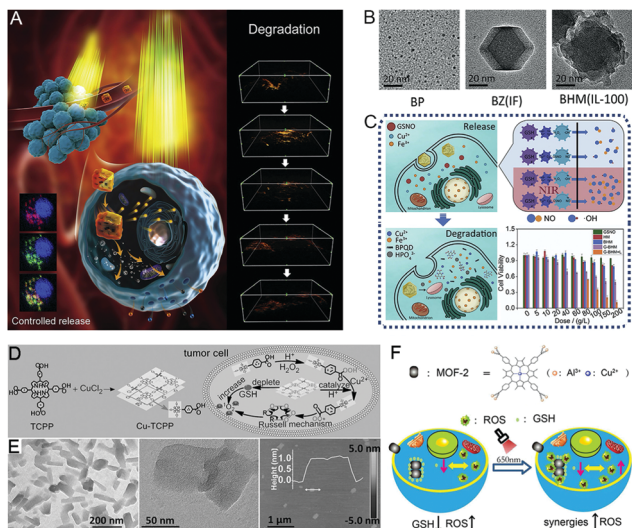


**Fig. 2** Copper-based nMOFs. (A) A schematic illustration, (B) TEM images, and (C) the mechanism of action of BHM for biodegradable multimodal therapy. Reproduced with permission.<sup>30</sup> Copyright: 2019, Elsevier Ltd. (D) Preparation procedure and (E) characterization of Cu-TCPP nanosheets for Russell-mechanism-induced selective catalytic theranostics. Reproduced with permission.<sup>31</sup> Copyright: 2019, Wiley-VCH. (F) The mechanism of  $(\text{CuL}-[\text{AlOH}]_2)_n$  for GSH-depletion-enhanced PDT. Reproduced with permission.<sup>32</sup> Copyright: 2018, Wiley-VCH.

unique GSHOx-mimicking performance of Cu-based nMOFs has also been well established.

As shown in Fig. 2A–C, black phosphorous quantum dots (BP QDs) were encapsulated into a nanoscale multicomponent (Cu and Fe)-based nMOF (BHM) to achieve a multimodal therapy.<sup>30</sup> Encouragingly, the rationally designed BHM was reported not only to stimulate the production of  $\cdot\text{OH}$  and nitric oxide (NO), but also to achieve drug loading and imaging. In addition, BP QDs could trigger hyperthermia under near-infrared (NIR) laser irradiation to accelerate the formation of  $\cdot\text{OH}$  and NO. Another study on intracellular GSH-consuming

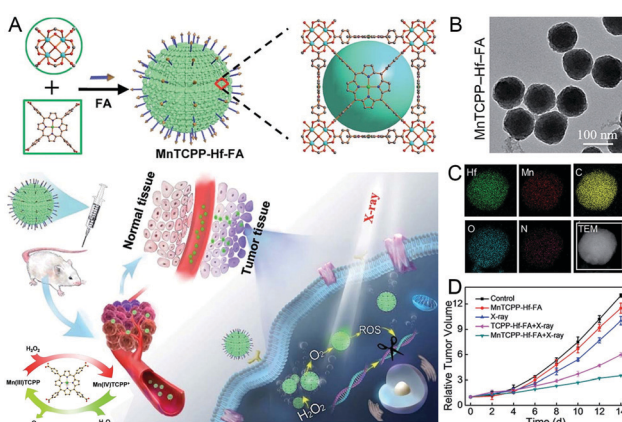


**Fig. 3** Manganese-based nMOFs. (A) The preparation procedure, (B and C) characterization, and (D) tumor volume in diverse treatment groups of CAT-mimicking MnTCPP-Hf-FA nMOFs. Reproduced with permission.<sup>35</sup> Copyright: 2019, Royal Society of Chemistry.

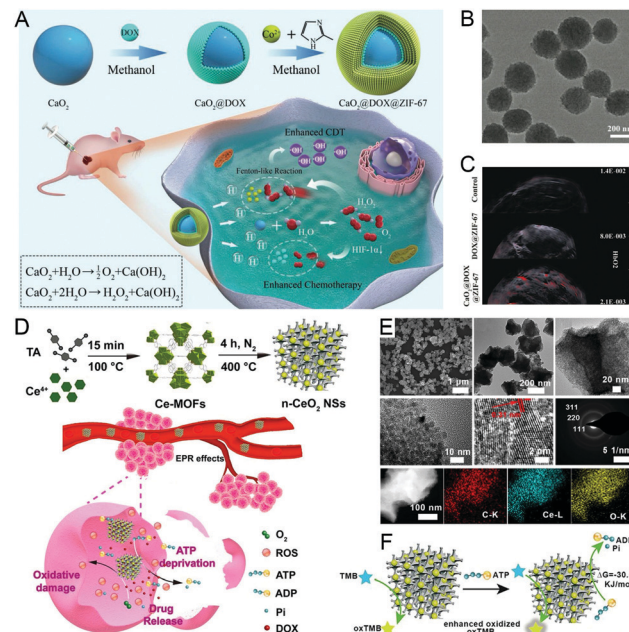


**Fig. 4** Cobalt-/cerium-based nMOFs. (A) A schematic illustration, (B) TEM images and (C) PAI of  $\text{CaO}_2@\text{DOX}@ZIF-6$  for combined chemo-/catalytic-therapy. Reproduced with permission.<sup>36</sup> Copyright: 2019, Wiley-VCH. (D) Mechanism of action, (E) characterization, and (F) oxidative-damage- and reduced-energy-supply-enabled Ce-based nMOFs. Reproduced with permission.<sup>37</sup> Copyright: 2018, American Chemical Society.

ultrathin two-dimensional (2D) Cu-based nMOFs nanosheets ( $\text{Cu-TCPP}$ ; TCPP = tetrakis(4-carboxyphenyl)porphyrin, a photosensitizer) was reported by Wang *et al.* (Fig. 2D and E).<sup>31</sup> In TME instead of normal tissues, the Cu-TCCP nanosheets could generate ROS *via* the Russell mechanism, which was proved to be feasible even under low oxygen conditions and without the introduction of external NIR light. In addition, as a promising novel PDT candidate,  $\text{Cu}^{2+}$ -metalated nMOFs ( $\text{CuL}-[\text{AlOH}]_2)_n$  (Fig. 2F) exhibited comparable therapeutic efficacy to that of a commercial chemo-agent (camptothecin, CPT).<sup>32</sup> This GSHOx-mimicking nMOF possessed considerable intracellular GSH depletion ability, thus synergistically increasing the efficacy of the produced ROS to accelerate apoptosis.

### 2.3 Manganese-based nMOFs

Mn-based nMOFs, possessing Mn ions with different valences, have previously been developed for magnetic resonance imaging.<sup>33</sup> More importantly, the unique Mn-based nMOFs that were distinguished by CAT-mimicking activity have shown their potential as excellent therapeutic agents for relieving the hypoxia of tumors.

Recently, Mn<sup>2+</sup>-based nMOFs were designed for catalytic therapy to alleviate the limitations of tumor hypoxia for enhanced-PDT.<sup>34</sup> These nMOFs could effectively increase  $\text{O}_2$  concentration by Mn<sup>2+</sup> catalysis and generate ROS by TCPP porphyrins in a hypoxic solid tumor. In another study, MnTCPP-Hf-FA was constructed as a CAT-mimicking radiosensitizer for tumor-targeted radiotherapy (Fig. 3A–D).<sup>35</sup> As a high- $z$

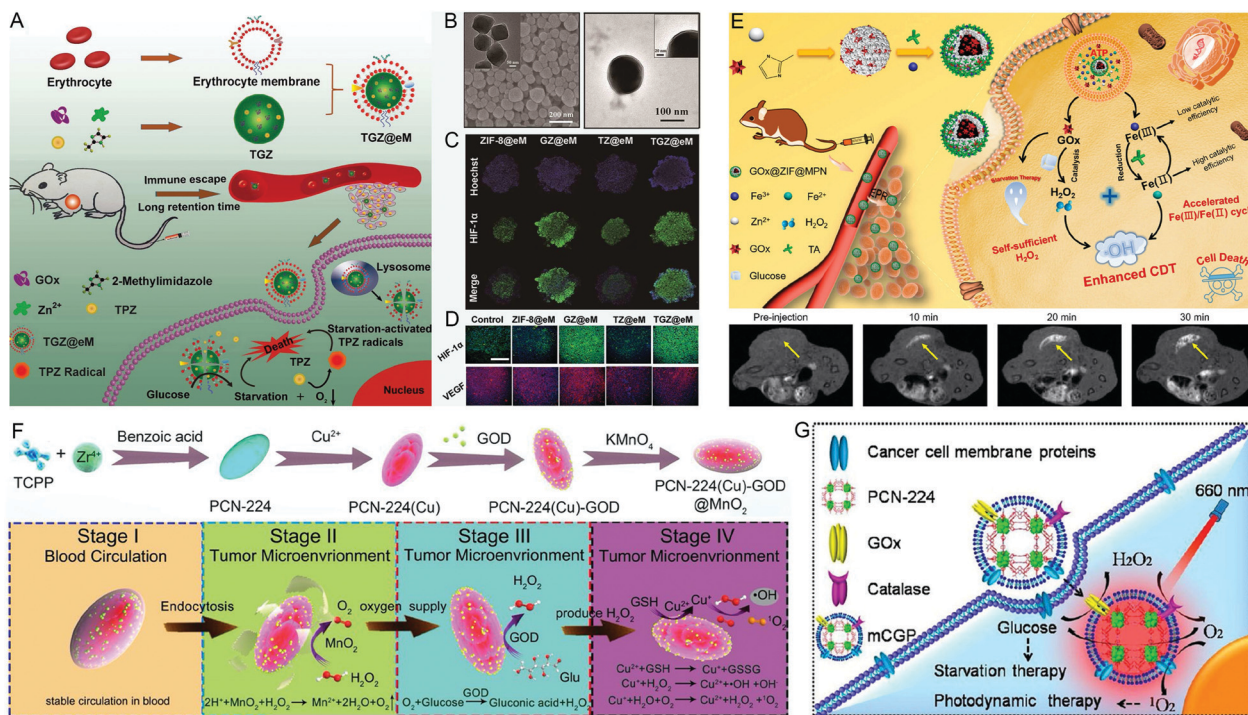


**Fig. 5** Glucose oxidase-engineered nMOFs. The (A) preparation and (B) characterization of TGZ and TGZ@eM. (C) The heterogeneity of the TME with a hypoxic region and (D) tumor tissue staining from mice under various treatments. Reproduced with permission.<sup>16</sup> Copyright: 2018, American Chemical Society. (E) A schematic illustration of the preparation, anti-tumor action, and MRI imaging of GOx@ZIF@MPN. Reproduced with permission.<sup>42</sup> Copyright: 2018, American Chemical Society. (F) The synthesis and application of PCN-224(Cu)-GOx@MnO<sub>2</sub>. Reproduced with permission.<sup>43</sup> Copyright: 2020, American Chemical Society. (G) A schematic illustration of mCGP as a cascade bioreactor for tumor-targeted starvation and PDT. Reproduced with permission.<sup>46</sup> Copyright: 2017, American Chemical Society.

element, hafnium (Hf) clusters were applied to produce ROS under X-ray irradiation to induce cell apoptosis. Combining catalytic and radiotherapy capabilities, this nanosystem could achieve *in situ* O<sub>2</sub>-production and relieve hypoxia-induced radioresistance to prevent postoperative recurrence of tumors.

#### 2.4 Cobalt-based nMOFs

Co-Based nanomaterials feature low toxicity, low cost, a flexible nanostructure design and functionalization strategies. Therefore, intelligent nMOFs based on Co with enzyme-mimicking activity can be employed for catalytic therapy. For example, doxorubicin (DOX) and calcium peroxide (CaO<sub>2</sub>) were successfully co-encapsulated in a Co-based nanosized zeolitic imidazole framework (ZIF-67) as a nanocatalytic medicine (CaO<sub>2</sub>@DOX@ZIF-67) (Fig. 4A–C).<sup>36</sup> Under weakly acidic conditions, CaO<sub>2</sub> in the absence of ZIF-67 protection could react with H<sub>2</sub>O to self-supply O<sub>2</sub> and H<sub>2</sub>O<sub>2</sub>. The as-generated O<sub>2</sub> and H<sub>2</sub>O<sub>2</sub> further improved the chemotherapy efficacy of DOX and promoted the Fenton-like reaction mediated by Co<sup>2+</sup>, which therefore optimized the effectiveness of combined chemo/catalytic therapy.

#### 2.5 Cerium-based nMOFs

As a lanthanide compound, Ce-based nanomaterials process broad applications in the fields of electrochemistry, magnetism and catalysis. Ce has been employed with different organic

ligands to form nMOFs with novel properties. In this regard, excellent OXD-mimicking Ce-based nMOFs were fabricated *via* a one-step method, in which the ultrasmall homogeneous cerium oxide (n-CeO<sub>2</sub>) nanoparticles were isolated (Fig. 4D–F).<sup>37</sup> The OXD-like and adenosine triphosphate (ATP) deprivation capacities endowed these nanostructures with excellent oxidative damage and blocked energy supply effects. By virtue of their admirable catalytic hydrolysis activity on ATP, these nanostructures could blaze a new path for synergistic tumor treatment with negligible side effects.

### 3. Enzyme-engineered nMOFs

Natural enzymes are proteins with high specificity and high catalytic efficiency for substrates, which are widely used in food, medicine, the chemical industry, and other fields. However, enzymes are not stable enough, and may perform with insufficient catalytic activity without post-modification. Preparation of enzyme-nMOFs composites by using the unique frame structures of nMOFs is one of the methods used to improve the stability of enzymes. Embedding the enzymes within or attaching them to the surface of nMOFs can effectively exploit the multiple functions of nMOFs with complementary catalytic ability. Recently, enzyme-engineered nMOFs have been introduced into the field of tumor diagnosis and

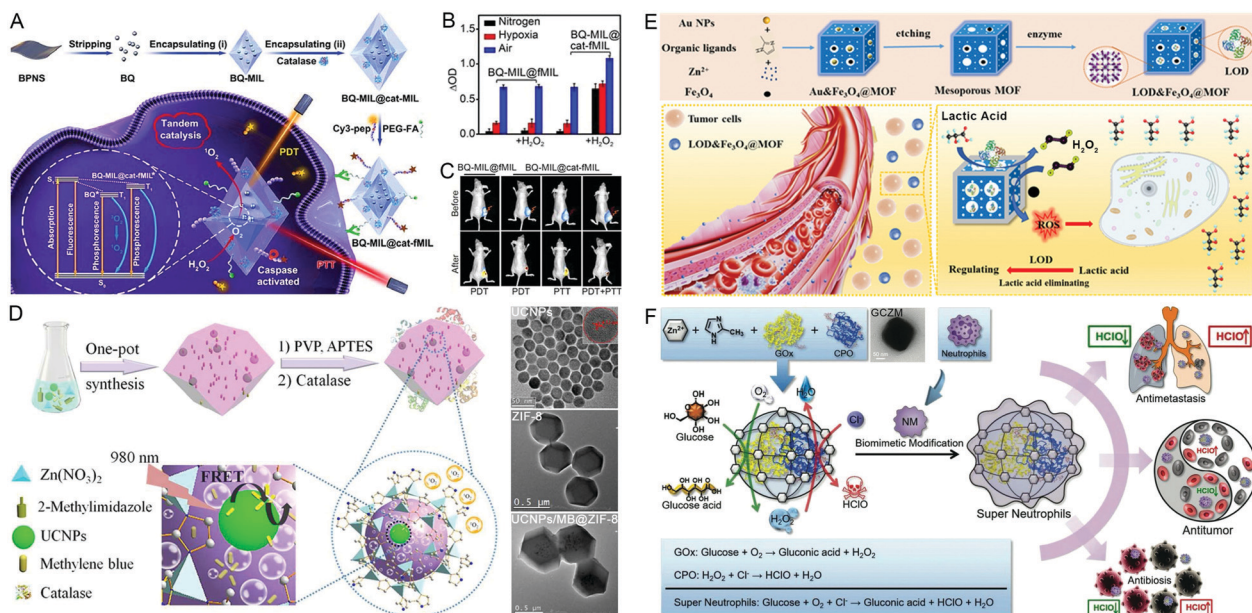


**Fig. 6** Catalase-engineered nMOFs. (A) The preparation, (B) PDT performance, and (C) tumor therapeutic efficacy of BQ-MIL@cat-fMIL.<sup>48</sup> Copyright: 2019, Wiley-VCH. (D) A schematic illustration of UCNPs/MB@ZIF-8@catalase preparation. Reproduced with permission.<sup>49</sup> Copyright: 2017, Royal Society of Chemistry. Lactate oxidase-engineered nMOFs. (E) The tandem biological-chemical catalytic reactions of LOD&Fe<sub>3</sub>O<sub>4</sub>@MOF for effective catalytic tumor treatment. Reproduced with permission.<sup>50</sup> Copyright: 2020, American Chemical Society. Chloroperoxidase-engineered nMOFs. (F) The fabrication, biomimetic reactions, and diverse biomedical applications of two enzyme (GOx and CPO)-embedded “super neutrophils.” Reproduced with permission.<sup>52</sup> Copyright: 2019, Wiley-VCH.

treatment. By catalyzing the overproduced  $\text{H}_2\text{O}_2$ , glucose and lactate in the TME, the promising TME-specific catalytic therapeutic performances of enzyme-engineered nMOFs in PDT/PTT/chemotherapy/radiotherapy have been improved.

### 3.1 Glucose oxidase-engineered nMOFs

The high glucose content in tumors provides sufficient nutrition for the rapid proliferation of tumor cells. Cancer starvation therapy refers to cutting off the supply of nutrients to cancer cells or depleting the oxygen in the tumor, thereby inhibiting the growth and proliferation of cancer cells.<sup>38–40</sup> However, single cancer-starvation therapy can prevent neither cancer metastasis nor recurrence, because the capillaries can continuously supply nutrients and oxygen for cancer cell proliferation.<sup>41</sup> During cancer treatment by the starvation strategy, nanomaterials carrying GOx can catalyze glucose to generate  $\text{H}_2\text{O}_2$  and gluconic acid, which consumes oxygen in the tumor microenvironment and further increases the hypoxia level. Therefore, some oxygen-dependent treatment methods (such as PDT or radiotherapy) will be hindered. Fortunately, CAT-like nanozymes can accelerate the decomposition of  $\text{H}_2\text{O}_2$  to generate  $\text{O}_2$ . In addition to the above-mentioned therapeutic strategies, researchers have also developed a variety of synergistic treatments in recent years, such as starvation and oxidation therapy, starvation and chemotherapy, or starvation and chemodynamic therapy.<sup>38</sup>

**Starvation and chemotherapy.** Zhang and colleagues developed GOx and hypoxia-triggered prodrug (tirapazamine, TPZ) co-loaded nMOFs which were encapsulated by an erythrocyte membrane (TGZ@eM) for synergistic starvation and chemotherapy

(Fig. 5A–D). In this nanoreactor, GOx was delivered to realize cancer starvation therapy, resulting in tumor hypoxia, further activating TPZ for enhanced chemotherapy. Furthermore, the biomimetic surface modification improved the targeting ability of nMOFs, and finally achieved TME-specific synergistic therapy.<sup>16</sup>

**Starvation and chemodynamic therapy.** In work by Zhang's group, ZIF-8 was used to encapsulate GOx, which was further coated with  $\text{Fe}^{3+}$  and a tannic acid (TA) shell (GOx@ZIF@MPN) (Fig. 5E).<sup>42</sup> After uptake by cancer cells, the GOx@ZIF@MPN would degrade to release  $\text{Fe}^{3+}$ , TA and GOx due to the presence of overexpressed ATP in the cancer cells. Then, GOx would catalyze the conversion of glucose to  $\text{H}_2\text{O}_2$ , while TA could promote the conversion of  $\text{Fe}^{3+}$  into  $\text{Fe}^{2+}$  to catalyze the self-produced  $\text{H}_2\text{O}_2$  to generate toxic  $\text{•OH}$ . Wang and colleagues applied fusiform-like  $\text{Cu}^{2+}$ -based nMOFs (PCN-224(Cu)-GOx@MnO<sub>2</sub>) for hypoxia relief and GSH-depletion co-enhanced starvation and Russell-mechanism-induced chemodynamic synergistic cancer therapy (Fig. 5F).<sup>43</sup> In another study, a cascade enzymatic/Fenton catalytic nanoplatform, Co-ferrocene MOF (Co-Fc nMOFs), was developed for starvation and chemodynamic synergistic therapy.<sup>44</sup> The Co-Fc nMOFs could increase the acidity and  $\text{H}_2\text{O}_2$  content in the tumor cells, which further promoted the performance of chemodynamic therapy.

**Starvation and photothermal therapy.** In a recent study, GOx and a photothermal agent (indocyanine green, ICG) were co-loaded into ZIF-8, which was further coated with a cancer cell membrane (CM) to develop GOx-ICG@ZIF@CM for synergistic starvation and PTT therapy.<sup>45</sup> Interestingly, two major defense proteins – catalase and monocarboxylate – that may

affect the starvation therapeutic effect of GOx, were down-regulated by ICG-mediated hyperthermia. Moreover, the expression of heat shock protein-90 which can guarantee the activation of proteins in hyperthermia would be inhibited by the starvation effect of GOx.

**Starvation and photodynamic therapy.** In a study that was conducted to explore the complementarity of starvation therapy and PDT, a cascade nanoreactor was successfully synthesized by attaching GOx and CAT on PCN-nMOFs (mCGP) (Fig. 5G).<sup>46</sup> Upon NIR laser irradiation, the generation of O<sub>2</sub> was accelerated in the presence of H<sub>2</sub>O<sub>2</sub>, subsequently producing <sup>1</sup>O<sub>2</sub>. In another study, a dual enzyme (GOx and CAT)-functionalized core-shell nanomotor based on nMOFs (UTZCG) was reported. The UCNPs were capable of generating toxic <sup>1</sup>O<sub>2</sub> for efficient PDT. The decomposition of H<sub>2</sub>O<sub>2</sub> could produce more O<sub>2</sub>, which could enhance the production of <sup>1</sup>O<sub>2</sub> and the consumption of intracellular glucose by GOx, resulting in efficient PDT and starvation therapy.<sup>47</sup>

### 3.2 Catalase-engineered nMOFs

CAT is commonly found in the liver and red blood cells of animals to decompose H<sub>2</sub>O<sub>2</sub> into H<sub>2</sub>O and O<sub>2</sub>. CAT-engineered nMOFs have been constructed for PDT or synergistic PDT/PTT against hypoxic tumors. For instance, BPQDs and CAT were encapsulated into nMOFs (BQ-MIL@cat-fMIL) through a step-wise *in situ* growth method (Fig. 6A–C).<sup>48</sup> The O<sub>2</sub> produced by CAT could not only alleviate the hypoxic environment of the tumor, but also greatly increase the efficiency of PDT. In addition, synergistic therapy was achieved by coupling with BQs-mediated PTT. In another study reported by Cai and colleagues, core-shell CAT-engineered and UCNPs (upconversion nanoparticles)-encapsulated nMOFs (UCNPs/MB@ZIF-8@catalase) were fabricated for NIR/H<sub>2</sub>O<sub>2</sub> responsive phototherapy (Fig. 6D), which showed excellent anti-tumor effects.<sup>49</sup>

### 3.3 Lactate oxidase-engineered nMOFs

The remarkable ability of tumor cells to uptake high amounts of glucose to maintain cell proliferation requirements, has been considered one of the hallmarks of a tumor. As a consequence of this energetic metabolism, also known as the “Warburg effect or aerobic glycolysis”, the excessive production of lactate is observed, leading to acidification of the extracellular pH in TME. The acidosis further favors several tumor-related processes, such as metastasis, angiogenesis and, more importantly, immunosuppression.

Impressively, lactic acid has been exploited to perform as a targeting molecule for various cancer modalities, among which transforming lactate in a tumor milieu into H<sub>2</sub>O<sub>2</sub> by lactate oxidase (LOD) shows broad applications. In this regard, hierarchical porous ZIF-8 was fabricated to co-load Fe<sub>3</sub>O<sub>4</sub> nanoparticles and LOD for lactate-responsive dual-modal catalytic therapy (Fig. 6E).<sup>50</sup> Identified as a target for TME regulation, lactic acid at tumor sites was depleted by embedding LOD which affected the cell cycle, further inducing apoptosis and tackling tumor cells. In parallel, the available generated H<sub>2</sub>O<sub>2</sub> was converted into <sup>1</sup>OH owing to the Fenton-like reaction

mediated by Fe<sub>3</sub>O<sub>4</sub> nanoparticles, which thus realized notable tandem catalysis. On the basis of lactate consumption and ROS killing as well as their synergy, such a nanocatalytic system initiated a powerful tumor suppression paradigm.

### 3.4 Chloroperoxidase-engineered nMOFs

Neutrophils, the first line of innate immune cells, are powerful effector leukocytes, which can migrate towards tumor tissue to ameliorate pathogen infections and oppose tumor progression. The mechanism of action of neutrophil-dependent cell inactivation is determined by the initial enzymatic oxidation of halide (e.g. Cl<sup>-</sup>) by H<sub>2</sub>O<sub>2</sub>, which can produce highly reactive hypochlorous acid (HClO) to destroy proteins or nucleic acids.<sup>51</sup>

Inspired by this distinct function, artificial “super neutrophil”-based enzymatic cascades are proposed by co-embedding GOx and chloroperoxidase (CPO, a robust peroxidase with higher resistance to oxidative inactivation) into ZIF-8 (denoted GCZM).<sup>52</sup> As illustrated in Fig. 6F, GCZM could generate a higher amount of reactive HClO for eradicating tumors and infections compared with that of natural neutrophils. The as-fabricated neutrophil-mimicking nanoplatform, featuring broad inflammation targeting and excellent tumor/pathogen eradication capability, demonstrated great potential for

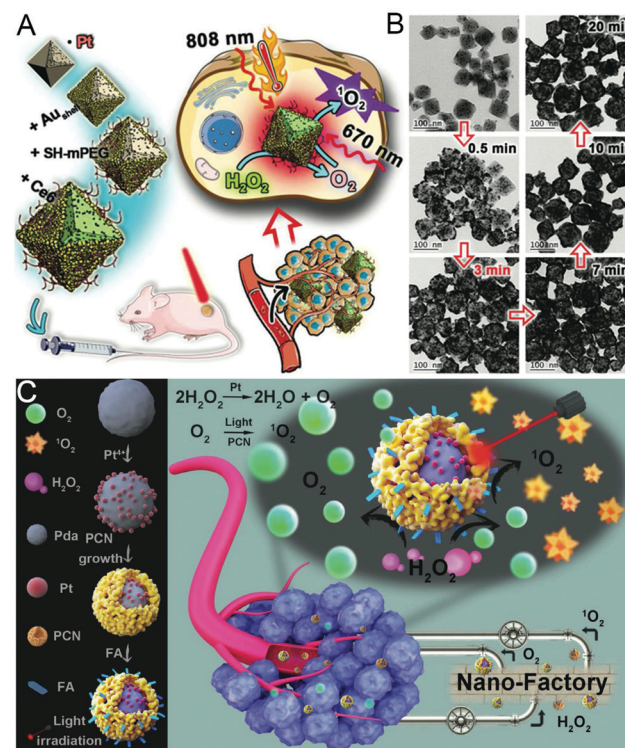


Fig. 7 Platinum nanozyme-engineered nMOFs. (A) A schematic illustration of PUA-Ce6 preparation and its application. (B) TEM images of porous gold nanoshells on nMOFs after different reaction times. Reproduced with permission.<sup>53</sup> Copyright: 2018, Wiley-VCH. (C) A schematic illustration of Pda-Pt@PCN-FA for enhanced tumor therapy. Reproduced with permission.<sup>54</sup> Copyright: 2018, Wiley-VCH.

diverse applications, including antitumor, anti-metastasis and antibiosis activities.

## 4. Nanozyme-engineered nMOFs

Compared to natural enzymes, nanozymes have been discovered with higher applicability, sufficient stability, and lower cost features.<sup>18</sup> Due to the unique physiochemical properties of nanozymes, they can be endowed with multiple functionalities to meet the wide requirements of a variety of applications. More importantly, the excessive operational demands during the fabrication of enzyme-based nanoplates, regarding the confined chemical reagents (usually water) and reaction temperatures (usually 37–40 °C to maintain enzymatic activity), might restrict the application of enzymes in the biomedicine field. In contrast, nanozymes could provide great opportunities for fabricating a variety of designable catalytic nanoplates without too much consideration of the reaction conditions. By coordinating or coating nanozymes with nMOFs, nanozyme-engineered nMOFs could be constructed to achieve TME-specific catalytic tumor therapy.

### 4.1 Platinum nanozyme-engineered nMOFs

CAT-mimicking platinum (Pt) nanozyme-engineered nMOFs are an excellent multi-functional tumor diagnosis and treatment platform. By combining catalytically active Pt nanozymes with multi-functional nMOFs, synergistic tumor treatment can

be achieved. For example, in recent work in our group, Pt nanozymes were encapsulated into NH<sub>2</sub>-MOFs and then further coated with porous gold nanoshells (PUA-Ce6) to achieve PTT in combination with O<sub>2</sub>-evolving-enhanced PDT (Fig. 7A and B).<sup>53</sup> In another study, a core-shell nanostructure with Pt NPs as interlayers and PCN nMOFs as the outer shell (Pda-Pt@PCN) was synthesized by Wang *et al.* (Fig. 7C).<sup>54</sup> The interference between O<sub>2</sub> production and <sup>1</sup>O<sub>2</sub> produced under light irradiation was effectively reduced due to the core-shell structure. A simple and general PDT enhancement strategy by decorating Pt nanozymes on PCN nMOFs (PCN-224-Pt) was reported by Zhang's group.<sup>55</sup> This nanoplate exhibits superior PDT enhancement efficiency under the cooperation of H<sub>2</sub>O<sub>2</sub> catalysis *via* Pt nanozymes.

### 4.2 Ultrasmall gold nanozyme-engineered nMOFs

Historically, gold (Au) has been labeled as being highly inert; however, nanosized gold materials have been discovered with multiple enzyme-mimicking activities in recent years, such as nuclelease, esterase, GOx, CAT, POD and superoxide dismutase. The catalytic activities of Au nanozymes are highly dependent on the surface states (naked or functionalized) and the morphologies (e.g. size and shape).<sup>56</sup> In the following subsections, we will highlight the catalytic activity of CAT- and GOx-mimicking abilities of ultrasmall Au NPs.

**Glucose oxidase-mimics.** Au NPs have the same stoichiometric reaction as GOx: that is, the reaction of glucose with O<sub>2</sub> and H<sub>2</sub>O to produce gluconic acid and H<sub>2</sub>O<sub>2</sub>.<sup>57,58</sup> Such activity

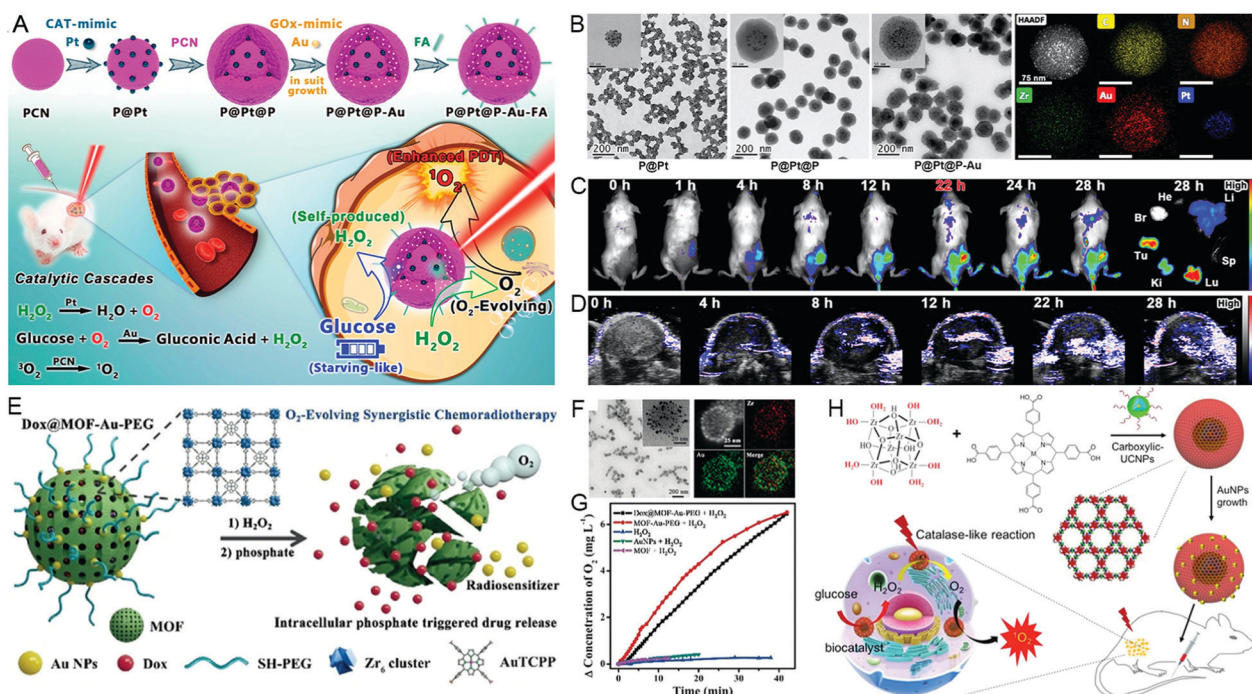


Fig. 8 Ultrasmall gold nanozyme-engineered nMOFs. (A) Fabrication process, and (B) TEM images and elemental mapping of P@Pt@P-Au. (C) *In vivo* fluorescence imaging and (D) oxygen saturation level after the i.v. injection of P@Pt@P-Au-FA at different time intervals. Reproduced with permission.<sup>59</sup> Copyright: 2019, American Chemical Society. (E) A schematic illustration and (F) the characterization of Dox@MOF-Au-PEG. (G) Oxygen generation in the presence of H<sub>2</sub>O<sub>2</sub>. Reproduced with permission.<sup>63</sup> Copyright: 2019, Wiley-VCH. (H) Core-shell UMOFs@Au NPs with dual enzyme-mimicking performance for enhanced PDT. Reproduced with permission.<sup>64</sup> Copyright: 2020, American Chemical Society.

of the GOx reaction might be consistent with that of the interaction between O<sub>2</sub> atoms and the surface of Au NPs. In a recent study by our group, dual-nanozyme-engineered PCN nMOFs (Fig. 8A–D) were constructed, in which the CAT-mimicking Pt NPs were sandwiched in the nMOFs and then embedded with surface-naked GOx-mimicking Au NPs (~2 nm) in the outer-shell layer (P@Pt@P-Au-FA) for catalytic-cascade-enhanced synergistic tumor therapy.<sup>59</sup> Furthermore, Fe-based nMOFs were doped with Au NPs to achieve starvation and chemodynamic therapy.<sup>60</sup> The constructed nMOFs could effectively protect the GOx-like activity of Au NPs by shielding the Au NPs from protein absorption. Therefore, the doped Au NPs could efficiently catalyze glucose in TME to produce H<sub>2</sub>O<sub>2</sub>, and to further react with Fe<sup>3+</sup> for the generation of highly toxic •OH.

**Catalase-mimics.** The possible mechanism of the CAT-mimicking ability of ultrasmall Au NPs was demonstrated by Jv and co-researchers.<sup>61</sup> The Au NPs at about 34 nm could adsorb H<sub>2</sub>O<sub>2</sub> on their surfaces, and double the generated •OH after O–O bond breaking. Meanwhile, the generated •OH might exchange partial electrons with the surface of the Au NPs to stabilize the CAT-like catalytic activity of Au NPs.<sup>62</sup> H<sub>2</sub>O<sub>2</sub> can be decomposed into •OH and O<sub>2</sub> at low and high pH conditions, respectively, which shows the controllable catalytic activity of Au NPs. In another study, a porphyrinic nMOFs–Au nanohybrid (Dox@MOF-Au-PEG) was constructed to achieve O<sub>2</sub>-evolving chemo-radiotherapy (Fig. 8E–G), in which the decorated Au NPs (with a size of less than 5 nm) could stabilize the nano-composite and sensitize radiotherapy.<sup>63</sup> Recently, core-shell UCNPs-encapsulated nMOFs nanoplatforms (UMOFs@Au NPs) were synthesized (Fig. 8H). The dual-enzyme mimicking ultrasmall Au NPs (~2 nm) could deplete glucose to produce H<sub>2</sub>O<sub>2</sub>, and thereafter supply O<sub>2</sub> via H<sub>2</sub>O<sub>2</sub> decomposition to achieve enhanced PDT.<sup>64</sup>

### 4.3 Manganese nanozyme-engineered nMOFs

In addition to Pt and ultrasmall Au nanozymes, CAT- and GSHOx-mimicking manganese nanozyme-engineered nMOFs have also been widely employed to effectively alleviate TEM for cancer treatment and diagnosis.<sup>65</sup> For instance, MnFe<sub>2</sub>O<sub>4</sub> nanozyme-engineered PCN nMOFs were proposed by Yin *et al.* for MRI-guided cancer theranostics (Fig. 9A–F).<sup>66</sup> The synthesized MnFe<sub>2</sub>O<sub>4</sub>@MOFs presented circulating catalysis of both CAT-mimicking and GSHOx-like activities, which could continuously achieve the decomposition of H<sub>2</sub>O<sub>2</sub> to generate O<sub>2</sub> in the tumor to overcome hypoxia, and also consume GSH in the presence of H<sub>2</sub>O<sub>2</sub> to reduce the consumption of ROS during PDT. In another study, apatinib (growth factor receptor 2 inhibitor)-loaded PCN nMOFs were coated with MnO<sub>2</sub> and a tumor cell membrane (aMMTm) for a combination of antiangiogenesis and PDT (Fig. 9G and H). The PDT efficiency was significantly improved in the presence of MnO<sub>2</sub>, proving their O<sub>2</sub>-generation and GSH-consumption abilities.<sup>67</sup> Moreover, apatinib was substantiated to neutralize the massive cell death and vasculature shutdown caused by PDT, thus effectively inhibiting tumor regrowth alongside metastasis.

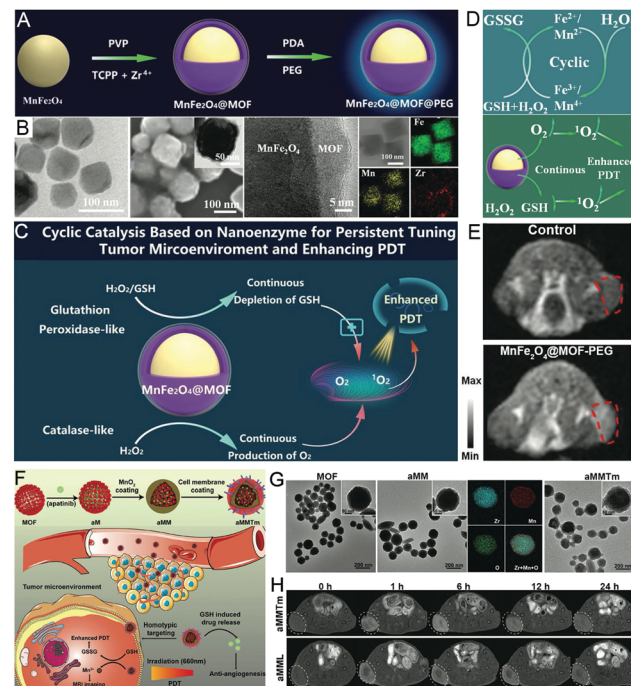


Fig. 9 Manganese nanozyme-engineered nMOFs. (A) The preparation process and (B) characterization of MnFe<sub>2</sub>O<sub>4</sub>@MOF. (C) A schematic illustration of MnFe<sub>2</sub>O<sub>4</sub>@MOF application. (D) Cyclic catalysis and (E) the MRI ability of MnFe<sub>2</sub>O<sub>4</sub>@MOF. Reproduced with permission.<sup>66</sup> Copyright: 2019, Wiley-VCH. (F) A schematic illustration of the application, (G) TEM images, and (H) the MRI ability of aMMTm. Reproduced with permission.<sup>67</sup> Copyright: 2018, Wiley-VCH.

## 5. Conclusions and perspectives

nMOF-mediated enzymatic chemical reactions for catalytic tumor-specific therapy have been gaining tremendous interest among the research community very recently, offering increasingly successful yields for preclinical oncology. Despite bearing unique properties and advantages, nMOF-based enzymatic nanocatalysts (nMOFs with intrinsic enzyme-mimicking performance, and enzyme- or nanozyme-engineered nMOFs) are still in their infancy, and several barriers to further progress remain to be addressed with respect to their prospective applications.

(1) **Biosafety concerns:** the toxicological compatibility and biodegradability of the metal ions and/or metal-containing nodes of nMOFs or the decorated nanozymes should be carefully evaluated. To date, metal ions with higher biocompatibility (*e.g.*, Fe, Zn, Zr, Mn, or Cu) are preferred and frequently applied to fabricate nMOF-based nanoreactors. In the meantime, the organic ligand-induced potential toxicity of nMOFs should also be considered. As for the enzymes that are employed for engineering nMOFs, severe systemic adverse effects should be critically evaluated.

(2) **Catalytic efficiency:** the POD-mimicking activities (Fenton and/or Fenton-like reactions) of nMOF-based nanozymes are severely suppressed in the presence of an insufficient H<sub>2</sub>O<sub>2</sub> supply in tumors. Besides, the TME (pH 6.5) also suffers from an unsatisfactory match with favorable pH requirements

(around 3–4) for triggering the effective production of  $\cdot\text{OH}$ . Interestingly, recent literature indicated that external stimuli (e.g., NIR-light-induced heat production) could improve the POD-mimicking activities of nanozymes. To this end, nMOF-based nanozymes with higher catalytic efficiency and less dependence on the catalytic environment are highly desirable.

(3) Immobilization of natural enzymes: although endowed with high catalytic efficiency and specificity, natural enzymes are proteins that demand confined chemical reagents and temperatures during the fabrication process. In addition, the immunogenicity and poor stability of enzymes also limit their further applications. Therefore, stable, efficient, and spatially controlled immobilization strategies for enzymes should be developed, rather than their simple decoration on the surfaces of nanomaterials *via* covalent conjugation or electrostatic interactions.

(4) nMOF-derived single-atom nanocatalysts: single-atom nanocatalysts (SACs), with respect to isolated metal centers with atomically dispersive activity sites anchored on solid supports, hold great promise for cost-effective catalysis.<sup>68</sup> The recent discovery of nMOFs serving as single-atom anchoring supports has tremendously fostered the development of SACs and presented brand-new breakthroughs for diverse applications.<sup>69–71</sup> Considering the diversity of metals and metal-containing organic ligands (e.g. Au, Pt) included in nMOFs, dual- or more-SACs-engineered nanoplatforms could be achieved on the basis of rationally designed nMOFs. In the foreseeable future, nMOF-derived single-atom nanocatalysts will further find use in enzymatic reactions for catalytic tumor-specific therapy.

In general, despite the highlighted challenges, nMOF-based enzymatic nanocatalysts have secured their place in tumor-specific therapy. Hopefully, this systematic review will provide potential directions to establish novel strategies for the development of next-generation catalytic nanomedicines, and will also spur further advances in nMOFs in nanomedicine as well as other technological spaces.

## Conflicts of interest

There are no conflicts to declare.

## Acknowledgements

This work was supported by the National Natural Science Foundation of China (31971292 and U1432114), Ministry of Science and Technology of the People's Republic of China (2018YFC0910601 and 2019YFA0405603) and Zhejiang Provincial Natural Science Foundation of China (LY18H180011).

## References

- 1 D. Hanahan and R. A. Weinberg, *Cell*, 2011, **144**, 646–674.
- 2 B. Yang, Y. Chen and J. Shi, *Chem. Rev.*, 2019, **119**, 4881–4985.
- 3 H. Lin, Y. Chen and J. Shi, *Chem. Soc. Rev.*, 2018, **47**, 1938–1958.
- 4 B. Yang, Y. Chen and J. Shi, *Adv. Mater.*, 2019, **31**, e1901778.
- 5 P. Zhu, Y. Chen and J. Shi, *ACS Nano*, 2018, **12**, 3780–3795.
- 6 H. Furukawa, K. E. Cordova, M. O'Keeffe and O. M. Yaghi, *Science*, 2013, **341**, 1230444.
- 7 L. Jiao, Y. Wang, H. L. Jiang and Q. Xu, *Adv. Mater.*, 2018, **30**, e1703663.
- 8 S. Dang, Q.-L. Zhu and Q. Xu, *Nat. Rev. Mater.*, 2017, **3**, 17075.
- 9 M. Zhao, K. Yuan, Y. Wang, G. Li, J. Guo, L. Gu, W. Hu, H. Zhao and Z. Tang, *Nature*, 2016, **539**, 76–80.
- 10 S. Zhao, Y. Wang, J. Dong, C.-T. He, H. Yin, P. An, K. Zhao, X. Zhang, C. Gao, L. Zhang, J. Lv, J. Wang, J. Zhang, A. M. Khattak, N. A. Khan, Z. Wei, J. Zhang, S. Liu, H. Zhao and Z. Tang, *Nat. Energy*, 2016, **1**, 16184.
- 11 X. Pan, L. Bai, H. Wang, Q. Wu, H. Wang, S. Liu, B. Xu, X. Shi and H. Liu, *Adv. Mater.*, 2018, **30**, e1800180.
- 12 M. X. Wu and Y. W. Yang, *Adv. Mater.*, 2017, **29**, e1606134.
- 13 K. Lu, T. Aung, N. Guo, R. Weichselbaum and W. Lin, *Adv. Mater.*, 2018, **30**, e1707634.
- 14 K. Lu, C. He, N. Guo, C. Chan, K. Ni, G. Lan, H. Tang, C. Pelizzari, Y. X. Fu, M. T. Spiotto, R. R. Weichselbaum and W. Lin, *Nat. Biomed. Eng.*, 2018, **2**, 600–610.
- 15 Y. Li, K. Zhang, P. Liu, M. Chen, Y. Zhong, Q. Ye, M. Q. Wei, H. Zhao and Z. Tang, *Adv. Mater.*, 2019, **31**, e1901570.
- 16 L. Zhang, Z. Wang, Y. Zhang, F. Cao, K. Dong, J. Ren and X. Qu, *ACS Nano*, 2018, **12**, 10201–10211.
- 17 D. Jiang, D. Ni, Z. T. Rosenkrans, P. Huang, X. Yan and W. Cai, *Chem. Soc. Rev.*, 2019, **48**, 3683–3704.
- 18 J. Wu, X. Wang, Q. Wang, Z. Lou, S. Li, Y. Zhu, L. Qin and H. Wei, *Chem. Soc. Rev.*, 2019, **48**, 1004–1076.
- 19 X. Lian, Y. Fang, E. Joseph, Q. Wang, J. Li, S. Banerjee, C. Lollar, X. Wang and H. C. Zhou, *Chem. Soc. Rev.*, 2017, **46**, 3386–3401.
- 20 B. Xu, H. Wang, W. Wang, L. Gao, S. Li, X. Pan, H. Wang, H. Yang, X. Meng, Q. Wu, L. Zheng, S. Chen, X. Shi, K. Fan, X. Yan and H. Liu, *Angew. Chem., Int. Ed.*, 2019, **58**, 4911–4916.
- 21 S. Wang, L. Shang, L. Li, Y. Yu, C. Chi, K. Wang, J. Zhang, R. Shi, H. Shen, G. I. Waterhouse, S. Liu, J. Tian, T. Zhang and H. Liu, *Adv. Mater.*, 2016, **28**, 8379–8387.
- 22 Q. Xia, H. Wang, B. Huang, X. Yuan, J. Zhang, J. Zhang, L. Jiang, T. Xiong and G. Zeng, *Small*, 2019, **15**, e1803088.
- 23 Z. Tang, Y. Liu, M. He and W. Bu, *Angew. Chem., Int. Ed.*, 2019, **58**, 946–956.
- 24 H. Ranji-Burachaloo, P. A. Gurr, D. E. Dunstan and G. G. Qiao, *ACS Nano*, 2018, **12**, 11819–11837.
- 25 F. Liu, L. Lin, Y. Zhang, Y. Wang, S. Sheng, C. Xu, H. Tian and X. Chen, *Adv. Mater.*, 2019, **31**, e1902885.
- 26 B. Yang, L. Ding, H. Yao, Y. Chen and J. Shi, *Adv. Mater.*, 2020, **32**, e1907152.
- 27 G. Lan, K. Ni, Z. Xu, S. S. Veroneau, Y. Song and W. Lin, *J. Am. Chem. Soc.*, 2018, **140**, 5670–5673.
- 28 T. Zhang, Z. Jiang, L. Chen, C. Pan, S. Sun, C. Liu, Z. Li, W. Ren, A. Wu and P. Huang, *Nano Res.*, 2020, **13**, 273–281.
- 29 N. Yang, W. Xiao, X. Song, W. Wang and X. Dong, *Nano-Micro Lett.*, 2020, **12**, 15.
- 30 T. Y. Du, Z. J. Qin, Y. K. Zheng, H. Jiang, Y. Weizmann and X. M. Wang, *Chem*, 2019, **5**, 2942–2954.

31 C. Wang, F. J. Cao, Y. D. Ruan, X. D. Jia, W. Y. Zhen and X. E. Jiang, *Angew. Chem., Int. Ed.*, 2019, **58**, 9846–9850.

32 W. Zhang, J. Lu, X. Gao, P. Li, W. Zhang, Y. Ma, H. Wang and B. Tang, *Angew. Chem., Int. Ed.*, 2018, **57**, 4891–4896.

33 W. Tang, W. Fan, W. Zhang, Z. Yang, L. Li, Z. Wang, Y. L. Chiang, Y. Liu, L. Deng, L. He, Z. Shen, O. Jacobson, M. A. Aronova, A. Jin, J. Xie and X. Chen, *Adv. Mater.*, 2019, **31**, e1900401.

34 J. Lu, L. Yang, W. Zhang, P. Li, X. Gao, W. Zhang, H. Wang and B. Tang, *Chem. Commun.*, 2019, **55**, 10792–10795.

35 Y. Chen, H. Zhong, J. Wang, X. Wan, Y. Li, W. Pan, N. Li and B. Tang, *Chem. Sci.*, 2019, **10**, 5773–5778.

36 S. Gao, Y. Jin, K. Ge, Z. Li, H. Liu, X. Dai, Y. Zhang, S. Chen, X. Liang and J. Zhang, *Adv. Sci.*, 2019, **6**, 1902137.

37 F. Cao, Y. Zhang, Y. Sun, Z. Wang, L. Zhang, Y. Huang, C. Liu, Z. Liu, J. Ren and X. Qu, *Chem. Mater.*, 2018, **30**, 7831–7839.

38 L. H. Fu, C. Qi, Y. R. Hu, J. Lin and P. Huang, *Adv. Mater.*, 2019, **31**, e1808325.

39 L. H. Fu, C. Qi, J. Lin and P. Huang, *Chem. Soc. Rev.*, 2018, **47**, 6454–6472.

40 M. Wang, D. Wang, Q. Chen, C. Li, Z. Li and J. Lin, *Small*, 2019, **15**, e1903895.

41 X. Zhang, G. Li, D. Wu, X. Li, N. Hu, J. Chen, G. Chen and Y. Wu, *Biosens. Bioelectron.*, 2019, **137**, 178–198.

42 L. Zhang, S. S. Wan, C. X. Li, L. Xu, H. Cheng and X. Z. Zhang, *Nano Lett.*, 2018, **18**, 7609–7618.

43 Z. Wang, B. Liu, Q. Sun, S. Dong, Y. Kuang, Y. Dong, F. He, S. Gai and P. Yang, *ACS Appl. Mater. Interfaces*, 2020, **12**, 17254–17267.

44 C. Fang, Z. Deng, G. Cao, Q. Chu, Y. Wu, X. Li, X. Peng and G. Han, *Adv. Funct. Mater.*, 2020, **30**, 1910085.

45 P. Gao, M. Shi, R. Wei, W. Pan, X. Liu, N. Li and B. Tang, *Chem. Commun.*, 2020, **56**, 924–927.

46 S. Y. Li, H. Cheng, B. R. Xie, W. X. Qiu, J. Y. Zeng, C. X. Li, S. S. Wan, L. Zhang, W. L. Liu and X. Z. Zhang, *ACS Nano*, 2017, **11**, 7006–7018.

47 Y. You, D. Xu, X. Pan and X. Ma, *Appl. Mater. Today*, 2019, **16**, 508–517.

48 J. Liu, T. Liu, P. Du, L. Zhang and J. Lei, *Angew. Chem., Int. Ed.*, 2019, **58**, 7808–7812.

49 H. J. Cai, T. T. Shen, J. Zhang, C. F. Shan, J. G. Jia, X. Li, W. S. Liu and Y. Tang, *J. Mater. Chem. B*, 2017, **5**, 2390–2394.

50 X. Zhou, W. Zhao, M. Wang, S. Zhang, Y. Li, W. Hu, L. Ren, S. Luo and Z. Chen, *ACS Appl. Mater. Interfaces*, 2020, **12**, 32278–32288.

51 Q. Wu, Z. He, X. Wang, Q. Zhang, Q. Wei, S. Ma, C. Ma, J. Li and Q. Wang, *Nat. Commun.*, 2019, **10**, 240.

52 C. Zhang, L. Zhang, W. Wu, F. Gao, R. Q. Li, W. Song, Z. N. Zhuang, C. J. Liu and X. Z. Zhang, *Adv. Mater.*, 2019, **31**, e1901179.

53 C. Liu, L. Luo, L. Zeng, J. Xing, Y. Xia, S. Sun, L. Zhang, Z. Yu, J. Yao, Z. Yu, O. U. Akakuru, M. Saeed and A. Wu, *Small*, 2018, **14**, e1801851.

54 X.-S. Wang, J.-Y. Zeng, M.-K. Zhang, X. Zeng and X.-Z. Zhang, *Adv. Funct. Mater.*, 2018, **28**, 1801783.

55 Y. Zhang, F. Wang, C. Liu, Z. Wang, L. Kang, Y. Huang, K. Dong, J. Ren and X. Qu, *ACS Nano*, 2018, **12**, 651–661.

56 Y. Lin, J. Ren and X. Qu, *Adv. Mater.*, 2014, **26**, 4200–4217.

57 M. Comotti, C. Della Pina, R. Matarrese and M. Rossi, *Angew. Chem., Int. Ed.*, 2004, **43**, 5812–5815.

58 S. Gao, H. Lin, H. Zhang, H. Yao, Y. Chen and J. Shi, *Adv. Sci.*, 2019, **6**, 1801733.

59 C. Liu, J. Xing, O. U. Akakuru, L. Luo, S. Sun, R. Zou, Z. Yu, Q. Fang and A. Wu, *Nano Lett.*, 2019, **19**, 5674–5682.

60 X. Liu, Y. Pan, J. Yang, Y. Gao, T. Huang, X. Luan, Y. Wang and Y. Song, *Nano Res.*, 2020, **13**, 653–660.

61 Y. Jv, B. Li and R. Cao, *Chem. Commun.*, 2010, **46**, 8017–8019.

62 J. Li, W. Liu, X. Wu and X. Gao, *Biomaterials*, 2015, **48**, 37–44.

63 Z. He, X. Huang, C. Wang, X. Li, Y. Liu, Z. Zhou, S. Wang, F. Zhang, Z. Wang, O. Jacobson, J. J. Zhu, G. Yu, Y. Dai and X. Chen, *Angew. Chem., Int. Ed.*, 2019, **58**, 8752–8756.

64 L. He, Q. Ni, J. Mu, W. Fan, L. Liu, Z. Wang, L. Li, W. Tang, Y. Liu, Y. Cheng, L. Tang, Z. Yang, Y. Liu, J. Zou, W. Yang, O. Jacobson, F. Zhang, P. Huang and X. Chen, *J. Am. Chem. Soc.*, 2020, **142**, 6822–6832.

65 Y. Chen, Z. H. Li, P. Pan, J. J. Hu, S. X. Cheng and X. Z. Zhang, *Adv. Mater.*, 2020, **32**, e2001452.

66 S. Y. Yin, G. Song, Y. Yang, Y. Zhao, P. Wang, L. M. Zhu, X. Yin and X. B. Zhang, *Adv. Funct. Mater.*, 2019, **29**, 1901417.

67 H. Min, J. Wang, Y. Qi, Y. Zhang, X. Han, Y. Xu, J. Xu, Y. Li, L. Chen, K. Cheng, G. Liu, N. Yang, Y. Li and G. Nie, *Adv. Mater.*, 2019, **31**, e1808200.

68 B. Qiao, A. Wang, X. Yang, L. F. Allard, Z. Jiang, Y. Cui, J. Liu, J. Li and T. Zhang, *Nat. Chem.*, 2011, **3**, 634–641.

69 D. Wang, H. Wu, S. Z. F. Phua, G. Yang, W. Qi Lim, L. Gu, C. Qian, H. Wang, Z. Guo, H. Chen and Y. Zhao, *Nat. Commun.*, 2020, **11**, 357.

70 L. Jiao, H. Yan, Y. Wu, W. Gu, C. Zhu, D. Du and Y. Lin, *Angew. Chem., Int. Ed.*, 2020, **59**, 2565–2576.

71 M. Huo, L. Wang, Y. Wang, Y. Chen and J. Shi, *ACS Nano*, 2019, **13**, 2643–2653.